JOURNAL OF NANO- AND ELECTRONIC PHYSICS
Vol. **5** No 4, 04033(3pp) (2013)

ЖУРНАЛ НАНО- ТА ЕЛЕКТРОННОЇ ФІЗИКИ
Том **5** № 4, 04033(3cc) (2013)

Short Communication

Physico-Chemical Properties of Nanoparticles Functionalized by Polypyrrole

Yu.A. Mirgorod, V.M. Fedosyuk, N.A. Borsch

[1] *Southwest State University, 94, 50 let Octyabrya Str. 305040 Kursk, Russian Federation*
[2] *SSPA "Scientific-Practical Materials Research Centre of NAS of Belarus", Institute of Solid State Physics and semiconductors of NAS of Belarus*

(Received 07 October 2013; published online 10 December 2013)

Magnetite nanoparticles coated with polypyrrole have been synthesized. Nanocomposite powder has been investigated by FTIR, XRD, SEM, magnetometry, conductivity measurements. Polypyrrole in nanocomposite does not impair the magnetic properties of magnetite.

Keywords: Magnetite, Polypyrrole, FTIR, XRD, SEM, Magnetometry, Conductivity measurements.

PACS number: 81.16.Be

1. INTRODUCTION

The formation of sub-micron particles, which have many useful properties, is necessary for effective technological applications. Such multifunctional nanoscale composites often have the structure of core-shell particles. They are synthesized, studied and used in medicine, diagnostics, biomedical science, and cells separation. Fe_3O_4 nanoparticles have good superparamagnetic properties. They are used for cancer cells hyperthermia, precise drug delivery, imaging of the objects of the human body [1]. To expand biotechnological application of Fe_3O_4 nanoparticles, functionalization of their surface which can be achieved, in particular, using polypyrrole is of importance. Polypyrrole has good biocompatibility and high electrical conductivity. It is easy to functionalized both by drugs and biologically active agents [2].

When combining Fe_3O_4 nanoparticles (NPM) and polypyrrole (PP), it is important to find out the changes in the magnetic properties of NPM and the conductive properties of PP. We report here about the synthesis of Fe_3O_4 nanoparticles coated with polypyrrole (NPM @ PP), and physico-chemical properties of inorganic and organic nanocomposite.

2. METHODS AND MATERIALS

For the synthesis of NPM, PP, NPM @ PP, chemically pure $Fe_2(SO4)_3 \cdot 9H_2O$, $Fe(SO_4) \cdot 7H_2O$, pyrrole, and oleic acid produced by Sigma were used.

8.6 g of $Fe_2(SO_4)_3 \cdot 9H_2O$ and 2.235 g of $Fe(SO_4) \cdot 7H_2O$ were dissolved in 200 ml of distilled water and stirred with a magnetic stir bar under nitrogen transmission. Then a mixture of 20 ml of concentrated ammonium hydroxide, 2 ml of oleic acid and 30 ml of water was gradually added dropwise to this solution. The resulting solution was heated to 90 °C and stirred for 30 min. Gradually black precipitate of NPM settled out. The precipitate was separated by centrifugation, decanted, then washed with water and decanted, then washed with ethanol and decanted, air dried and then oven dried at 60-70 °C.

The resultant NPM (0.6803 g) were stirred in 100 ml of 0.06 M solution of $Fe_2(SO_4)_3 \cdot 9H_2O$ (3.37 g) (the catalyst of pyrrolepolymerization). 0.02 M pyrrole (1.38 ml) was added dropwise into the solution. The solution gradually darkened as a result of the derivatization of PP. The reaction mixture was stirred during 3 hours. The dark precipitate NPM@PP was filtered. The precipitate of nanocomposite was washed with ethanol, dried in vacuum desiccator for 1 hour, then air dried for 15-16 hours. The weight ratio of magnetite to PP in NPM @ PP powder was 1.5.

The diffraction patterns (XRD) of NPM, PP and NPM@PP powders were recorded on X-ray diffractometer Dron-4 with CuK radiation ($\lambda = 0.154$ nm) with a step of 0.02° and a step time interval 1.25 sec. IR spectra of the powders were obtained using the spectrometer Nicolet iS50. The sizes of powders particles were investigated with the scanning electron microscope JEOL 6610LV. The magnetic properties of the powders were measured using the ponderomotive method [3]. ZFC-FC curves of nanopowders were received using Cryogenic high field measurement system [4]. The resistance of PP and NPM @ PP powders was measured on a precision meter LCR-7821 in the pressed sample.

3. EXPERIMENTAL RESULTS AND DISCUSSION

The morphology of the powders is shown on the scanning electron microscope images (Fig. 1). The PP particles are of various sizes, while the NPM@PP particles represent a conglomerate of smaller NPM, covered with cottonous PP.

FTIR- spectra of NPM have an absorption frequency of 575 cm^{-1}, that is a characteristic feature of Fe-O stretching vibrations. NPM@PP and PP show the

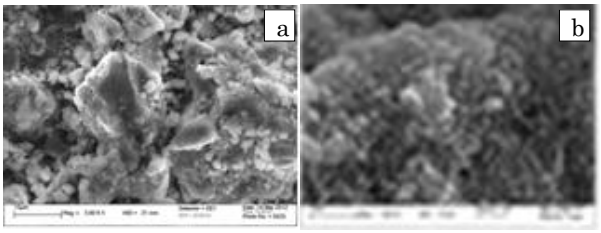

Fig. 1 – Scanning electron microscope images: a – polypyrrole, b – NPM@PP composite

The article was reported at the International Conference «Physics and Technology of Nanomaterials and Structures», Kursk, 21-22 November, 2013

same frequencies 3430 (deformation vibrations N-H), 1604 (C = N and N-H), 1024 cm^{-1} (C-H bond). The spectra confirm the production of polypyrrole, Fe_3O_4 and absence of differences, and, thus, absence of chemical interactions of NPM and PP in the NPM@PP structure to form metal-ligand bonds.

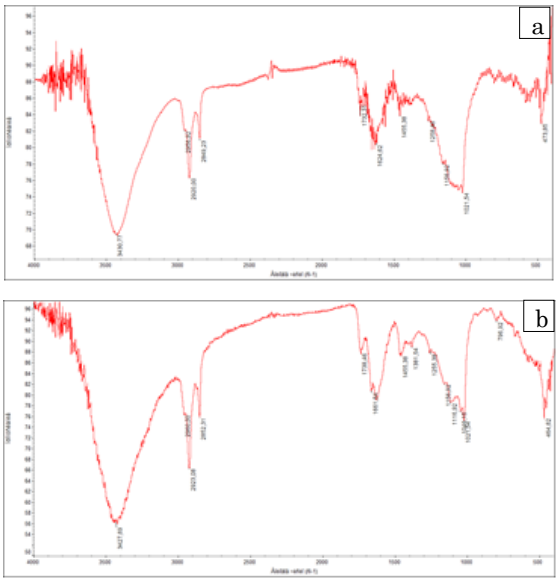

Fig. 2 – FTIR – powders spectra: a– polypyrrole, b – NPM @ PP

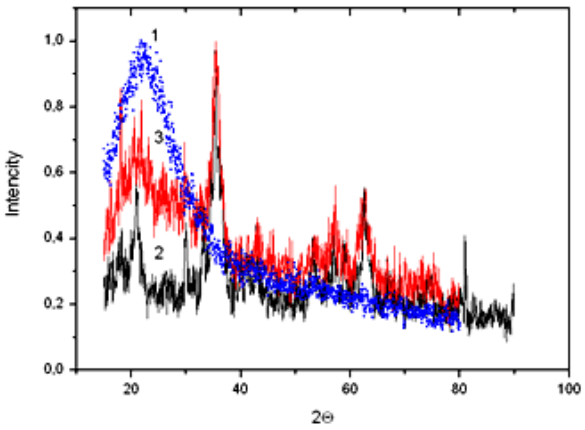

Fig. 3 – The diffraction patterns of powders: 1 – polypyrrole, 2 – NPM@PP, 3 – NPM

XRD diagram of NPM confirms the crystalline cubic spinel structure of Fe_3O_4 according to the standard JCPDS 85-1476 and the NPM size of 20 nm calculated according to Scherer formula (Fig. 3). All reflexes of NPM and NPM@PP coincide with each other. Consequently, the crystal structure of NPM when covered with a layer of an organic polymer does not change. XRD investigation shows that PP powder is in a greater degree amorphous with a small content of the crystalline phase. Wide reflex observed at the angle of $2 = 24°$ appears due to the reflection from the surfaces on which there are the polymer chains of PP. The average distance between the surfaces can be calculated using the relationship [5]

$$S = 5\lambda / 8\sin\theta, \qquad (1)$$

where S is the distance between chains, is the diffraction angle at the maximum intensity of the amorphous halo. The calculated average S is 0.45 nm. XRD diagram is used to calculate the average size of PP crystallites by Scherer formula

$$D = k\lambda / \rho\cos\theta, \qquad (2)$$

where D is the crystallite size, k is the shape factor which is assumed to be 0.89, if the crystallite shape is unknown, is the width at the half maximum of the diffraction angle in radians, $2\theta = 24°$. For PP powder according to the equation (2) D is 53 nm.

Similar NPM@PP diagram had reflexes NPM and PP with intensities corresponding to the composition (Fig. 3). For example, the intensity ratio of $2\theta = 24°$ NPM and NPM@PP is equal to (1.5).

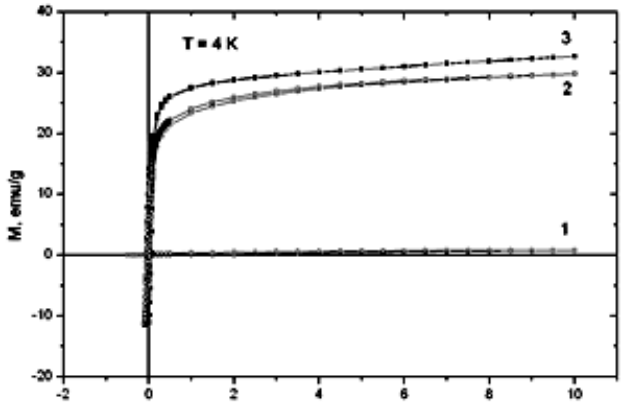

Fig. 4 – The specific magnetization of powders depending on the strength of the applied magnetic field: 1 – polypyrrole, 2 – NPM@PP, 3 – NPM

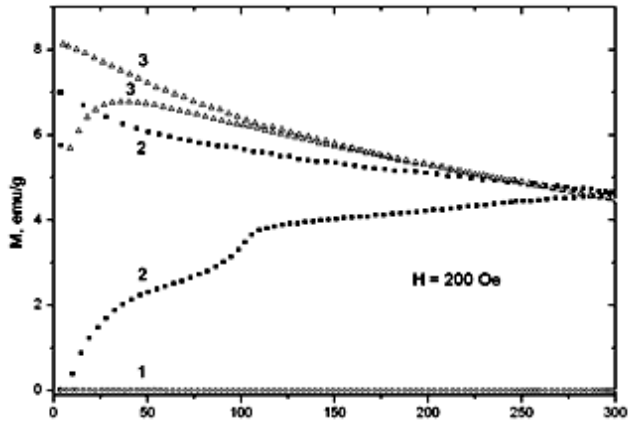

Fig. 5 – ZFC and FC curves of powders at a constant magnetic field strength: 1 – polypyrrole, 2 – NPM@PP, 3 – NPM

The specific magnetization of saturation of NPM@PP 27 $A \cdot m^2 \cdot kg^{-1}$ is slightly smaller than that of NPM (Fig. 4), and its dependence on the potential gradient has a shape common to superparamagnetics as there is no residual magnetization or coercive force. PP has almost zero magnetization. However, its low magnetization almost does not change the magnetization of NPM@PP compared to NPM. The specific magnetization of saturation of NPM Ms, defined by Fig. 3 is 35 $A \cdot m^2 \cdot kg^{-1}$.

To determine the temperature dependence of the specific magnetization two types of measurements were performed: in the cooled zero-magnetic-field (ZFC) and in the cooled non-zero-magnetic-field (FC) [5]. In the ZFC technique (Fig. 5), the sample was cooled to the temperature of liquid helium in the absence of magnetic field, and then a small magnetic field H = 300 Oe was enabled and the temperature was being slowly increased and specific magnetization was being registered. FC technique differed only in that the powder sample was cooled in a non-zero-magnetic-field H = 300 Oe.

As can be seen, the curves of ZFC and FC at NPM coincide at certain temperatures, but start to differ below a certain reversibility temperature TH = 150 K. Besides, ZFC curve has its maximum (T_{max}) at blocking temperature TB = 45 K, and FC curve grows monotonically up to the lowest temperatures. The value of TH can be identified with TB of the particles of maximum size and the value of T_{max} can be identified with TB of the particles of minimum size. The critical diameter for the room temperature of the NPM single-domain spherical particle with axial magnetic anisotropy is 128 nm [5]. In experimental studies at TB the abrupt change in magnetization never occurs because there is a spread of the particles in size. In this case the spread is assumed to be between 20-130 nm.

A large difference between the ZFC and FC curves at NPM@PP, and a small difference at NPM can be because of the coherence of small particles of magnetite in NPM@PP by polypyrrole (Fig. 5). The size of the nanoparticles increases and NPM@PP particles demonstrate the characteristics of ferromagnetic behavior instead of superparamagnetic one.

The resistance of NPM@PP pressed powders at room temperature was 70-75 kOhm. PP conductivity at 30 °C was 70 kOhm, and at 40 °C it was 64 kOhm that matches the other investigators [6] and it was a little different from NPM@PP composite. Electrical conductivity increased with the temperature. This indicates the thermally-activated mechanism of electrical conductivity of polypyrrole, i.e. the increase of the efficiency of charge transfer with the increase of temperature.

4. CONCLUSIONS

Thus, magnetic and conductive properties of the composite core-shell NPM@PP almost do not change compared to NPM and PP, and the surface of the composite can be functionalized, giving new biological properties.

REFERENCES

1. H.W. Yang, M.Y. Hua, H.L. Liu, C.Y. Huang, K.C. Wei, *Nanotechnology, Science and Application* **5**, 73 (2012).
2. A. Nan, R. Turcu, I. Bratu, C. Leostean, O. Chauvet, E. Gautron. J. Liebscher, *Arkivoc*. **10**, 185 (2010).
3. S.G. Yemelyanov, Yu.A. Mirgorod, V.M. Fedosyuk, *Izvestiya Yugo-Zapadnogo Gosudarstvennogo Universiteta* **43**, No4, 115 (2012).
4. Yu.A. Mirgorod, N.A. Borshch, V.M. Fedosyuk, G.Yu. Yurkov *Inorg. Mater.* **49**, 109 (2013).
5. S.P. Gubin, Yu.A. Koksharov, G.B. Khomutov, G.Yu. Yurkov *Russ. Chem. Rev.* **74**, 489 (2005).
6. K. Cheach, M. Forsyth, V.T. Truong. *Sinthetic Metal.* **101**, 19 (1999).